Int. J. Heat Mass Transfer. Vol. 31, No. 6, pp. 1211–1219, 1988
Printed in Great Britain

0017–9310/88 $3.00+0.00

Theory of heat transfer-irreversible power plants

ADRIAN BEJAN
Department of Mechanical Engineering and Materials Science, Duke University, Durham, NC 27706, U.S.A.

(*Received* 9 *September* 1987 *and in final form* 3 *November* 1987)

Abstract—The observed degree of thermodynamic imperfection of existing power plants is explained based on a steady-state power plant model the irreversibility of which is due to three sources: the hot-end heat exchanger, the cold-end heat exchanger and the heat leaking through the plant to the ambient. While maximizing the instantaneous power output, it is shown that in addition to Curzon and Ahlborn's optimum temperature ratio there exists also an optimum balance between the sizes of the hot- and cold-end heat exchangers. A graphic construction for pinpointing the optimum location of the power plant on the absolute temperature scale is presented. The efficiency (first or second law) is maximum when the total investment is split optimally between the external conductance and internal thermal resistance built into the power plant. The efficiency data on existing power plants fall in the domain anticipated theoretically. Some of the trade-offs revealed by the theory are illustrated further by the analysis of an ideal Brayton cycle power plant.

INTRODUCTION

THE GENERATION of mechanical power is the original mission of the science of engineering thermodynamics and much of the heat transfer engineering practiced today. It would be easy to argue that the world has come a long way from the early steam engines and reciprocating machinery that got the field started. One could also argue that the major post-Watt technological breakthroughs in power generation triggered their own, new brands of power engineering. There is of course truth in this argument, as even a quick glance at the library shelf invites the reader to think of the beginnings of more specialized modern fields, for example, internal combustion engines, turbomachinery, jet propulsion, etc. Yet I will argue that of more fundamental importance is what links all these developments rather than what sets them apart. The technological developments that led to today's explosive growth in electrical power production are all manifestations of a common design philosophy.

In this paper I rely on a very simple heat transfer model in order to anticipate the degree of thermodynamic irreversibility that is demonstrated by the power plants that have been built. This theory reveals also the existence of three fundamental trade-offs in the design of a power plant. The greater objective of this paper is to draw attention to the emergence of a science of irreversible power and refrigeration systems, as a research-active field in modern thermal engineering. This new direction is the modern counterpart of the Carnot-limit arguments which in the last century gave birth to classical thermodynamics. The field of irreversible power plants to which this paper contributes is the result of the interaction between classical thermodynamics and the now mature science of heat and mass transer. It is the latter that gives the thermodynamicist a firm grip on the irreversibilities that plague the present and future power and refrigeration systems.

IRREVERSIBLE POWER PLANT MODEL

Consider the model outlined in Fig. 1. The power plant delineated by the solid boundary operates between the high temperature T_H and low temperature T_L. The modeling challenge consists of providing the minimum construction detail that allows the outright identification of the irreversible and reversible compartments of the power plant.

In order to see the reasoning behind some of the features included in this drawing it is worth recalling that in the traditional treatment of simple power plant models (e.g. the Carnot cycle) it is tacitly assumed that the heat engine is in perfect thermal equilibrium with each temperature reservoir during the respective heat transfer interactions. In reality, however, such equilibria would require either an infinitely slow cycle or infinitely large contact surfaces between the engine and the reservoirs (T_H and T_L). For this reason the existence of the finite temperature differences $(T_H - T_{HC})$ and $(T_{LC} - T_L)$ is recognized as driving forces for the instantaneous heat transfer interactions $\dot{Q}_{HC}$ and $\dot{Q}_{LC}$

$$\dot{Q}_{HC} = C_H(T_H - T_{HC}) \tag{1}$$

$$\dot{Q}_{LC} = C_L(T_{LC} - T_L). \tag{2}$$

The proportionality coefficients C_H and C_L are the hot- and cold-end thermal conductances. In heat exchanger design terms, for example, C_H represents the product of the hot-end heat transfer area A_H times the overall heat transfer coefficient based on that area, $\bar{h}_H$. Since both C_H and C_L are commodities

NOMENCLATURE

a	temperature ratio, equation (51)
A	heat transfer area
c_P	specific heat at constant pressure
c_v	specific heat at constant volume
C_e	external conductance inventory
C_H	external conductance of the hot-end heat exchanger
C_i	internal conductance
C_L	external conductance of the cold-end heat exchanger
C_t	total conductance investment constraint
$\bar{h}$	overall heat transfer coefficient
k	ratio of specific heats, c_P/c_v
$\dot{m}$	mass flow rate
M	dimensionless mass flow rate, $\dot{m}c_P/(\bar{hA})$
N_H	heater number of heat transfer units, equation (52)
N_L	cooler number of heat transfer units, equation (52)
p_e	unit cost of external conductance
p_r	unit cost of internal resistance
P_H	high pressure
P_L	low pressure
$\dot{Q}_H$	heating rate
$\dot{Q}_{HC}$	heating rate to the reversible part of the power plant model
$\dot{Q}_i$	internal heat leak
$\dot{Q}_L$	cooling or heat rejection rate
$\dot{Q}_{LC}$	heat rejection rate from the reversible part of the power plant model
R_i	internal thermal resistance
$\dot{S}_{gen}$	entropy generation rate
T	absolute temperature
T_H	high temperature
T_{HC}	high temperature experienced by the reversible part of the power plant model
T_L	low (ambient) temperature
T_{LC}	low temperature experienced by the reversible part of the power plant model
$\dot{W}$	power output
x	external conductance (C_e) allocation ratio
y	total conductance (C_t) allocation ratio.

Greek symbols

η_C	Carnot efficiency, equation (31)
η_I	first-law efficiency, equation (29)
η_{II}	second-law efficiency, equation (30)
π	price ratio number, equation (41)
τ	temperature ratio, T_H/T_L
τ_C	Carnot temperature ratio, T_{HC}/T_{LC}.

Subscripts

C	reversible (Carnot) part of the power plant model
H	high, or hot end
L	low, or cold end
max	maximum
opt	optimum.

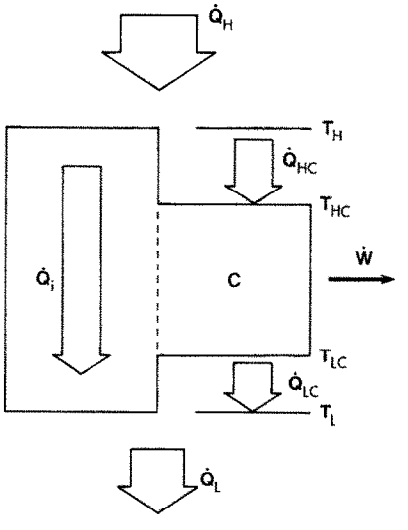

FIG. 1. Power plant model with three sources of heat transfer irreversibility (the power plant is delineated by the solid boundary).

in short supply it makes sense to recognize as a constraint the total external conductance inventory C_e

$$C_e = C_H + C_L \tag{3}$$

or, by introducing the external conductance allocation ratio x

$$C_H = xC_e \tag{4}$$

$$C_L = (1-x)C_e. \tag{5}$$

The heat transfer rates that cross the finite temperature gaps identified above represent two sources of irreversibility. A third source sketched in Fig. 1 is the heat transfer rate $\dot{Q}_i$ that leaks directly through the machine and, especially, around the power producing compartment labeled C. In order to distinguish this third irreversibility from the 'external' irreversibilities due to $(T_H - T_{HC})$ and $(T_{LC} - T_L)$, refer to $\dot{Q}_i$ as the 'internal' heat transfer rate (heat leak) through the plant. There are many features of an actual power plant that fall under the umbrella represented by $\dot{Q}_i$, for example, the heat transfer lost through the wall of a boiler or combustion chamber, the heat transfer removed by the cooling system of an internal combustion engine, and the streamwise convective heat leak channeled towards room temperature by the counterflow heat exchanger of a regenerative Brayton

cycle [1]. The simplest internal heat leak model that is consistent with the linear models, equations (1) and (2), is

$$\dot{Q}_i = C_i(T_H - T_L) \tag{6}$$

where C_i is the internal conductance of the power plant. Worth noting is that the internal heat leak model, equation (6), was proposed first in Problem 2.2 on p. 44 of ref. [1].

To summarize the three irreversibility sources that have already been discussed, note that the model of Fig. 1 relies analytically on three parameters, namely (C_H, C_L, C_i) or (C_e, x, C_i). The remaining power plant compartment, which is C, is irreversibly free. The second law of thermodynamics states that its rate of entropy generation is zero, which means that

$$\frac{\dot{Q}_{LC}}{T_{LC}} - \frac{\dot{Q}_{HC}}{T_{HC}} = 0. \tag{7}$$

The analytical representation of Fig. 1 is completed by the first-law statements

$$\dot{W} = \dot{Q}_{HC} - \dot{Q}_{LC} \tag{8}$$

$$\dot{Q}_H = \dot{Q}_i + \dot{Q}_{HC} \tag{9}$$

$$\dot{Q}_L = \dot{Q}_i + \dot{Q}_{LC} \tag{10}$$

where $\dot{W}$, $\dot{Q}_H$ and $\dot{Q}_L$ are the energy rate interactions of the power plant as a whole, namely, the power output, the rate of heat input and the heat rejection rate.

TWO CONDITIONS FOR MAXIMUM POWER

Following the example set by Curzon and Ahlborn [2], attention is focused on the power output $\dot{W}$ with the objective of determining the conditions under which $\dot{W}$ is maximum. These conditions, it turns out, can be derived analytically in closed form. First, combining equations (8), (7) and (5) leads to

$$\dot{W} = (1-x)C_eT_L\left(\frac{T_{LC}}{T_L} - 1\right)\left(\frac{T_{HC}}{T_{LC}} - 1\right) \tag{11}$$

in which the unknown now is the ratio T_{LC}/T_L. From the second law, equation (7), and equations (4) and (5) it can be learned however that

$$\frac{T_{LC}}{T_L} = 1 - x + x\frac{\tau}{\tau_C} \tag{12}$$

where τ and τ_C are abbreviations for the actual temperature ratio and the Carnot-compartment temperature ratio

$$\tau = \frac{T_H}{T_L} \tag{13}$$

$$\tau_C = \frac{T_{HC}}{T_{LC}}. \tag{14}$$

Combining equations (11) and (12) yields

$$\dot{W} = x(1-x)C_eT_L\left(\frac{\tau}{\tau_C} - 1\right)(\tau_C - 1). \tag{15}$$

The above expression shows that the instantaneous power output per unit of external conductance inventory (constant C_e) can be maximized in two ways. Solving first $\partial\dot{W}/\partial\tau_C = 0$, the optimum Carnot-compartment temperature ratio is obtained

$$\tau_{C,opt} = \tau^{1/2} \tag{16}$$

and the corresponding power output maximum is

$$\dot{W}_{max} = x(1-x)C_eT_L(\tau^{1/2} - 1)^2. \tag{17}$$

It is important to note at this stage that equation (16) is the same as the equivalent temperature ratio result in Curzon and Ahlborn's theory [2], even though the latter was based on a somewhat different power plant model. Unlike the steady-state power plant model of Fig. 1, Curzon and Ahlborn's model covered one full cycle of the classical Carnot cylinder and piston apparatus in which the quasistatically compressed or expanded working fluid is not in thermal equilibrium with the reservoirs T_L and, respectively, T_H. More general treatments of the same problem have been published by Salamon *et al.* [3, 4], Salamon and Nitzan [5], and Andresen *et al.* [6]. The present model and the analysis leading to equation (16) is a noteworthy and more direct alternative for deriving equation (16). This simpler approach was pointed out by De Vos [7].

An entirely new aspect that is brought to light by the model of Fig. 1 is that there exists an optimum way to allocate the C_e inventory between the hot and cold ends, such that the power output is maximized once more. Setting the $\partial/\partial x$ derivative of expression (15) or (17) equal to zero yields the optimum external conductance allocation fraction

$$x_{opt} = \tfrac{1}{2}. \tag{18}$$

Substituting $x = x_{opt}$ in equation (17) gives the twice-maximized instantaneous power output

$$\dot{W}_{max,max} = \tfrac{1}{4}C_eT_L(\tau^{1/2} - 1). \tag{19}$$

In conclusion, in order to operate at maximum power there must be not only a 'balance' between the thermodynamic temperature ratios τ_C and τ, equation (16), but also a balance between the sizes of the hot- and cold-end heat exchangers. This second observation is particularly important because it adds to an analysis given earlier on pp. 145–147 of ref. [1], which, relative to a model equivalent to the right half of Fig. 1, showed that an additional unit of C_e induces a greater increase in $\dot{W}$ if it is invested in the cold-end heat exchanger. That analysis and its conclusions are the subject of certain restrictions, which are spelled out on p. 147 of ref. [1]. The optimum allocation rule, equation (18), gives another view of the problem of the most beneficial way for investing the additional unit of C_e. The choice between investing it in the

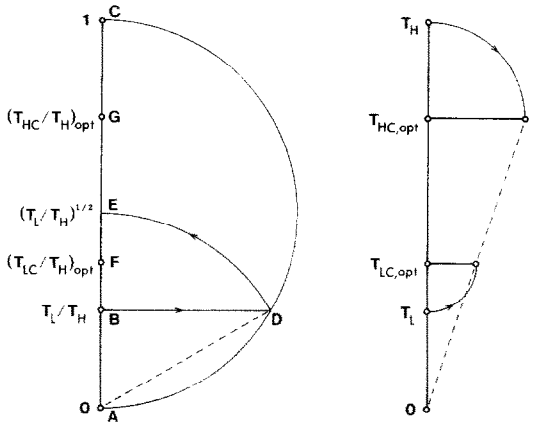

FIG. 2. Geometric construction for locating the optimum position of the power plant on the absolute temperature scale.

hot-end heat exchanger as opposed to the cold end depends on whether x is smaller than x_{opt} or not. If the two heat exchangers are already optimally balanced, $x = x_{opt}$, then the best way to invest the additional unit of C_e is by splitting it evenly between the two heat exchangers.

It can be noted finally that in heat transfer terms the double act of $\dot{W}$ maximization developed in this section is the same as choosing the optimum temperature differences of the two heat exchangers. It can be shown that when $\tau_C = \tau_{C,opt}$ and $x = x_{opt}$ these two temperature differences are

$$\left(\frac{T_H - T_{HC}}{T_H}\right)_{opt} = \tfrac{1}{2}(1-\tau^{-1/2}) \tag{20}$$

$$\left(\frac{T_{LC} - T_L}{T_L}\right)_{opt} = \tfrac{1}{2}(\tau^{1/2}-1) \tag{21}$$

or, after dividing equations (20) and (21)

$$\left(\frac{T_H - T_{HC}}{T_{LC} - T_L}\right)_{opt} = \tau^{1/2}. \tag{22}$$

In conclusion, the optimum end temperature differences are in the same proportion as the optimum temperatures felt by the Carnot part of the power plant, equation (16).

CONSTRUCTION OF THE TEMPERATURE SCALE

The two maximum $\dot{W}$ conditions of the preceding section are summarized most succinctly by the geometric construction presented on the left-hand side of Fig. 2. This construction begins with the observation that, when T_H and T_L are specified, the double maximization of $\dot{W}$ pinpoints the location of T_{HC} and T_{LC} on the absolute temperature scale. Let the temperature interval between T_H and absolute zero be represented by the segment of unit length $\overline{CA}$. On this segment the position of the low temperature reservoir is known (called point B), and it can be noted that the length of the segment $\overline{BA}$ equals T_L/T_H. The problem reduces to finding the position of points G and F. The solution is obtained by using no more than a compass and an unmarked ruler.

(1) Draw the unit-length circle having $\overline{CA}$ as diameter, and intersect it with the horizontal line drawn through B. Labeling the point of intersection D, recall a basic theorem of Pythagorean geometry which states that

$$\overline{BA} = \frac{(\overline{DA})^2}{\overline{CA}} \tag{23}$$

in other words, that the length of segment $\overline{DA}$ is equal to $(T_L/T_H)^{1/2}$. This new length is placed on the vertical axis by marking point E such that

$$\overline{EA} = \overline{DA}. \tag{24}$$

(2) Points G and F are located next as the midpoints of the new segments $\overline{CE}$ and, respectively, $\overline{EB}$, or by estimating the arithmetic average lengths

$$\overline{GA} = \tfrac{1}{2}(\overline{CA} + \overline{EA}) \tag{25}$$

$$\overline{FA} = \tfrac{1}{2}(\overline{EA} + \overline{BA}). \tag{26}$$

The latter are the geometric counterparts of two relations that follow from equations (20) and (21), namely

$$\left(\frac{T_{HC}}{T_H}\right)_{opt} = \frac{1}{2}\left[1 + \left(\frac{T_L}{T_H}\right)^{1/2}\right] \tag{27}$$

$$\left(\frac{T_{LC}}{T_H}\right)_{opt} = \frac{1}{2}\left[\left(\frac{T_L}{T_H}\right)^{1/2} + \frac{T_L}{T_H}\right]. \tag{28}$$

The right-hand side of Fig. 2 shows the four-temperature alignment produced by the geometric construction unveiled on the left-hand side. It is easier to see now that the optimum temperature differences $(T_H - T_{HC})_{opt}$ and $(T_{LC} - T_L)_{opt}$ are proportional to $T_{HC,opt}$ and, respectively, $T_{LC,opt}$. Indeed, by rotating these temperature difference segments by 90° one can see the emergence of two similar right triangles the common vertex of which is at the point of absolute zero.

ONE CONDITION FOR MAXIMUM EFFICIENCY

It remains to determine what sort of power plant 'efficiencies' are attainable with a design the focus of which has been on the maximization of the instantaneous production of power. The discussion can be carried out in terms of the traditional (first law) efficiency

$$\eta_I = \frac{\dot{W}}{\dot{Q}_H} \tag{29}$$

or, as done in this section, in terms of the second-law efficiency

$$\eta_{II} = \frac{\eta_I}{\eta_C} \tag{30}$$

where η_C is the Carnot efficiency associated with the temperature reservoirs T_H and T_L

$$\eta_C = 1 - \frac{T_L}{T_H}. \tag{31}$$

The second-law efficiency is known also as the rational or exergetic efficiency of the power plant [1, 8, 9]. It is a measure of the degree of thermodynamic irreversibility of the plant, that is, a measure of the departure from the fully-reversible limit represented by η_C. The range of possible values for η_{II} is 0–1 (Fig. 3).

The second-law efficiency that corresponds to the twice maximized power output, equation (19), is obtained by using equations (29)–(31) in combination with equation (9) for $\dot{Q}_H$, equation (6) for $\dot{Q}_i$ and equation (1) for $\dot{Q}_{HC}$, all subject to optimum conditions (16) and (18). The resulting expression is

$$\eta_{II} = \left[4\frac{C_i}{C_e}(1+\tau^{-1/2})^2 + 1 + \tau^{-1/2} \right]^{-1} \tag{32}$$

which shows that η_{II} depends on two parameters, the temperature ratio τ and the conductance ratio C_i/C_e. As one might have expected, the second-law efficiency decreases monotonically as the internal/external conductance ratio increases, i.e. as more of the heat transfer input $\dot{Q}_H$ is able to bypass the power producing part of the plant.

In search of the highest possible η_{II} one may think of increasing C_e and decreasing C_i, however, both moves are halted eventually by economic constraints. There exists an interesting trade-off between increasing C_e and increasing the internal thermal resistance $R_i = C_i^{-1}$, when the total resources available for both C_e and R_i are fixed. One can see that this trade-off corresponds to a minimum value of the ratio C_i/C_e, which in turn corresponds to a maximum value of the second-law efficiency η_{II}.

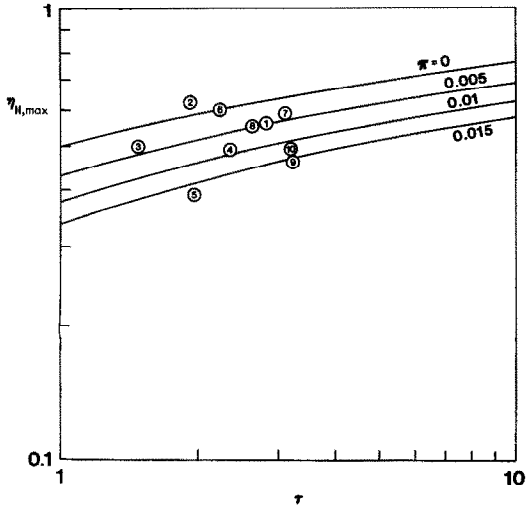

FIG. 3. Theoretical and empirical second-law efficiency data vs $\tau = T_H/T_L$ (the numbers inside the circles correspond to the numbers listed in the left-hand column of Table 1).

Assume that in the overall cost of the power plant C_e and R_i compete against one another in a cost constraint of the type

$$p_c C_e + p_r R_i = \text{constant} \tag{33}$$

where p_c and p_r are the unit costs (prices) associated with constructing more external conductance and, respectively, more internal resistance. Expressed in thermal conductance units constraint (33) reads

$$C_e + \frac{p_r}{p_c} R_i = C_t, \quad \text{constant} \tag{34}$$

where C_t is the total thermal conductance that could be built with the right-hand side of equation (33). The splitting of the total conductance inventory C_t between the actual external conductance and internal resistance is described by the investment allocation fraction y, which is defined by

$$C_e = yC_t \tag{35}$$

$$\frac{p_r}{p_c} R_i = (1-y)C_t. \tag{36}$$

Estimating now the C_i/C_e ratio in which C_t and p_r/p_c are considered fixed

$$\frac{C_i}{C_e} = \frac{p_r}{y(1-y)p_c C_t^2} \tag{37}$$

it is clear that this ratio reaches a minimum at

$$y_{opt} = \tfrac{1}{2} \tag{38}$$

and that its minimum value is

$$\left(\frac{C_i}{C_e}\right)_{min} = 4\frac{p_r/p_c}{C_t^2}. \tag{39}$$

The corresponding second-law efficiency maximum is

$$\eta_{II,max} = [16\pi(1+\tau^{-1/2})^2 + 1 + \tau^{-1/2}]^{-1} \tag{40}$$

in which π is the dimensionless notation for the price ratio parameter that came to light in equation (39)

$$\pi = \frac{p_r/p_c}{C_t^2}. \tag{41}$$

What has been achieved in equation (40) is a means to anticipate the ceiling value of η_{II} as a function of τ and the additional parameter π. The latter is not expected to vary much in any given technological age, therefore, it can be held constant while drawing each of the curves shown in Fig. 3. The second-law efficiency increases slowly as the temperature ratio increases. Even though, in principle, the entire 0–1 domain is accessible to η_{II}, the theory on which equation (40) is based suggests that the observed efficiencies of power plants must fall in the area *below* the $\pi = 0$ curve (recall that π is a positive finite number). The curve drawn for $\pi = 0$ represents the limit of infinitely plentiful internal resistance, for which equation (40) reduces to

Table 1. The observed efficiencies of ten power plants

Symbol on Fig. 3	Power plant	T_L (°C)	T_H (°C)	$\frac{T_H}{T_L}$	η_C	η_I	η_{II}
(1)	West Thurrock (U.K.), 1962 conventional coal fired steam plant [10]	25	565	2.82	0.64	0.36	0.56
(2)	CANDU (Canada), PHW nuclear reactor [11]	25	300	1.92	0.48	0.3	0.63
(3)	Larderello (Italy), geothermal steam plant [2,12]	80	250	1.48	0.32	0.16	0.5
(4)	1936–40 central steam power stations in the U.K. [10]	25	425	2.35	0.57	0.28	0.49
(5)	Calder Hall (U.K.), 1956 nuclear reactor [10]	25	310	1.96	0.49	0.19	0.39
(6)	Dungeness 'A' (U.K.), 1965 nuclear reactor [10]	25	390	2.23	0.55	0.33	0.60
(7)	1956 steam power plant in the U.S.A. [10]	25	650	3.1	0.68	0.40	0.59
(8)	1949 combined cycle (steam and mercury) plant in the U.S.A. [10]	25	510	2.63	0.62	0.34	0.55
(9)	1944 closed cycle gas turbine in Switzerland [10]	25	690	3.23	0.69	0.32	0.46
(10)	1950 closed cycle gas turbine in France [10]	25	680	3.20	0.69	0.34	0.49

$$\eta_{II,max}(\pi = 0) = \frac{\tau^{1/2}}{1+\tau^{1/2}}. \tag{42}$$

This limit is equivalent to the domain covered by Curzon and Ahlborn's theory [2], even though the second-law efficiency formula (42) does not appear in ref. [2]. Combining equation (42) with equation (30) it is easy to rederive Curzon and Ahlborn's first-law efficiency formula

$$\eta_I = 1 - \tau^{-1/2}. \tag{43}$$

I used the opportunity offered by the present theory to survey some of the second-law efficiency information available on power plants built during the past four decades (Table 1 and Fig. 3). With only one exception, the empirical η_{II} values fall under the $\pi = 0$ curve, that is, in a way that agrees with the present theory. This finding suggests that the simple model of Fig. 1 captures the most essential features of an actual power plant, that is, of a power plant that operates irreversibly.

Another interesting observation is that the second-law efficiencies of Table 1 correspond to a remarkably narrow band of π values. The average π value is approximately 0.01, which according to equation (39) corresponds to a C_i/C_e ratio of about 0.04. If, in addition, one regards $\tau \sim 2.5$ as representative of the τ values of the power plants of Table 1, one can learn that the $\dot{Q}_i/\dot{Q}_H$ ratio is roughly 12%.

This 'representative average' numerical example can be continued by asking the question of how (in what proportions) the three irreversibility mechanisms of Fig. 1 contribute to the aggregate irreversibility of the power plant. It turns out that when $\tau \sim 2.5$ and $C_i/C_e \sim 0.04$ the internal resistance contributes 40%, the hot-end external conductance 23% and the cold-end external conductance 37% of the overall entropy generation rate of the power plant.

AN IDEAL BRAYTON CYCLE EXAMPLE

The preceding conclusions were made to a large extent visible by the simplicity of the power plant model adopted in Fig. 1. More realistic power plant models—even the highly idealized ones—require more complex analytical and numerical work that tends to obscure the message conveyed by the preceding analysis. The mission of this section is to demonstrate that some of these trade-offs can be rediscovered in more realistic, textbook-type, power plant descriptions.

Consider for this purpose the ideal Brayton cycle sketched in Fig. 4. The working fluid (ideal gas with constant c_P) is heated at constant pressure (P_H) as it flows from the compressor outlet (1) to the turbine inlet (2). The compressor and the turbine process the fluid reversibly and adiabatically, i.e. isentropically. Between the turbine outlet (3) and the compressor inlet (4) the working fluid is cooled at constant pressure (P_L). The power plant is sandwiched between two temperature reservoirs, T_H and T_L, meaning that the maximum working fluid temperature can never exceed T_H, and that the minimum working fluid temperature can never fall below T_L. The Brayton cycle is said to be 'ideal' (or endoreversible) because the only irreversibilities accounted for by this model are external to the space occupied by the working fluid itself. These irreversibilities are associated with the heat transfer from T_H to the heater tube (1) → (2), and with the heat transfer from the cooler (3) → (4) to the low-temperature reservoir (T_L).

To maximize the instantaneous power output $\dot{W}$ is to minimize the entropy generation rate for the entire installation (cf. the Gouy–Stodola theorem on p. 24 of ref. [1])

$$\dot{S}_{gen} = \dot{m}c_P\left(\frac{T_3 - T_4}{T_L} - \frac{T_2 - T_1}{T_H}\right). \tag{44}$$

Note that this expression comes from writing

$$\dot{S}_{gen} = \frac{\dot{Q}_L}{T_L} - \frac{\dot{Q}_H}{T_H} \tag{45}$$

where

$$\dot{Q}_L = \dot{m}c_P(T_3 - T_4) \quad \text{and} \quad \dot{Q}_H = \dot{m}c_P(T_2 - T_1). \tag{46}$$

Alternatively, the overall entropy generation rate,

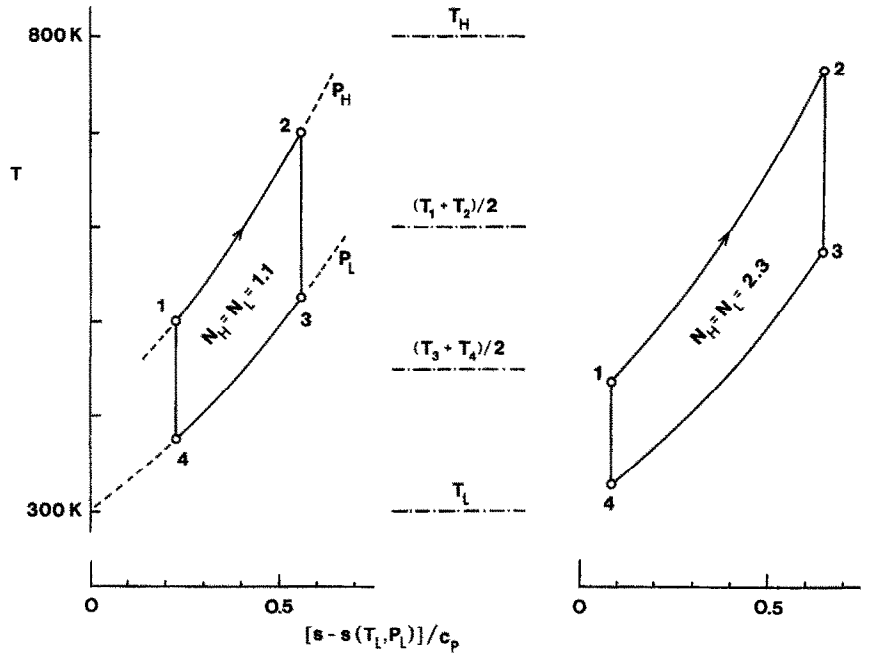

FIG. 4. Ideal Brayton cycle optimized for maximum power output (this figure was drawn to scale for the case $T_H = 800$ K, $T_L = 300$ K and the N_H and N_L values listed inside each cycle).

equation (44), may be derived by adding the contributions made by the two components that operate irreversibly

$$\dot{S}_{\text{gen},(T_H)-(\text{heater})} = \dot{m}c_P\left(\ln\frac{T_2}{T_1} - \frac{T_2-T_1}{T_H}\right) \quad (47)$$

$$\dot{S}_{\text{gen},(\text{cooler})-(T_L)} = \dot{m}c_P\left(\ln\frac{T_4}{T_3} - \frac{T_4-T_3}{T_L}\right). \quad (48)$$

The variation of the four corner temperatures $T_1, \ldots, T_4$ is constrained by four additional relations

$$\frac{T_H-T_1}{T_H-T_2} = e^{N_H} \quad (49)$$

$$\frac{T_3-T_L}{T_4-T_L} = e^{N_L} \quad (50)$$

$$\frac{T_1}{T_4} = \frac{T_2}{T_3} = a, \text{constant} \quad (51)$$

where the N's represent the 'number of heat transfer units' of each heat exchanger

$$N_H = \frac{(\bar{h}A)_H}{\dot{m}c_P}, \quad N_L = \frac{(\bar{h}A)_L}{\dot{m}c_P}. \quad (52)$$

Temperature ratio (51) depends only on the pressure ratio, $a = (P_H/P_L)^{(k-1)/k}$, where $k = c_P/c_v$. Finally, as a measure of the overall size of the heat exchanger equipment it is assumed that the total $(\bar{h}A)$ is fixed, which is analogous to equation (3). In the present terminology the $(\bar{h}A)$ constraint reads

$$N_H + N_L = \frac{(\bar{h}A)}{\dot{m}c_P} \quad (53)$$

where the flow rate $\dot{m}$ is not necessarily constant.

The overall entropy generation rate, equation (44), can be reshaped according to equations (49)–(53), to read

$$\frac{\dot{S}_{\text{gen}}}{(\bar{h}A)} = \frac{\dot{m}c_P}{(\bar{h}A)}\left[\left(\frac{T_H}{aT_L}\right)^{1/2} - \left(\frac{T_H}{aT_L}\right)^{-1/2}\right]^2 \times \frac{(e^{N_H}-1)(e^{N_L}-1)}{e^{N_H}e^{N_L}-1}. \quad (54)$$

This expression shows that $\dot{S}_{\text{gen}}$ decreases monotonically as the pressure ratio (a) increases, i.e. as the cycle expands vertically and eliminates the irreversibility plagued temperature gaps (note also that $\dot{S}_{\text{gen}}$ becomes zero in the limit $a = T_H/T_L$). Next, one can see that $\dot{S}_{\text{gen}}$ depends on both N_H and N_L, however only one of these parameters constitutes a degree of freedom (see equation (53)). It can be shown that the minimization of $\dot{S}_{\text{gen}}$ with respect to this single degree of freedom yields $N_H = N_L$, in other words, that

$$(\bar{h}A)_{H,\text{opt}} = (\bar{h}A)_{L,\text{opt}} = \tfrac{1}{2}(\bar{h}A) \quad (55)$$

$$\frac{\dot{S}_{\text{gen,min}}}{(\bar{h}A)} = \left[\left(\frac{T_H}{aT_L}\right)^{1/2} - \left(\frac{T_H}{aT_L}\right)^{-1/2}\right]^2 M\tanh\left(\frac{1}{4M}\right) \quad (56)$$

where M is the dimensionless shorthand for the mass flow rate, $M = \dot{m}c_P/(\bar{h}A)$. The same group ($M$) may be viewed as the inverse of the number of heat transfer units of the two heat exchangers combined. At large

flow rates ($M \gg 1$), the entropy generation rate minimum, equation (56), is practically independent of M, as the product M tanh $(1/4M)$ approaches 1/4. On the other hand, $\dot{S}_{\text{gen,min}}$ decreases proportionally with M when $M \ll 1$. In conclusion, there is a thermodynamic incentive for slowing down the working fluid as it bathes the two heat exchanger surfaces. In the limit $M = 0$ the extreme corners of the Brayton cycle match the imposed fuel and ambient temperatures, $T_2 = T_H$ and $T_4 = T_L$.

Either in terms of $(\bar{h}A)$ or number of heat transfer units, the optimum heat exchanger size distribution, equation (55), verifies the conclusion reached earlier on the basis of a much simpler power plant model, equation (18). The meaning of this design rule is illustrated in the remainder of Fig. 4. At the optimum, the arithmetic average temperature of the heater and the cooler depend solely on the imposed temperatures and pressures

$$(T_1 + T_2)_{\text{opt}} = T_H + aT_L \tag{57}$$

$$(T_3 + T_4)_{\text{opt}} = \frac{1}{a} T_H + T_L. \tag{58}$$

This conclusion matches in spirit the earlier result that the power cycle must occupy a certain position on the temperature scale between T_H and T_L (Fig. 2). Regardless of whether equation (55) applies, the heat engine efficiency is a function of P_H/P_L only

$$\eta_I = \frac{\dot{W}}{\dot{Q}_H} = 1 - \left(\frac{P_L}{P_H}\right)^{(k-1)/k} < 1 - \frac{T_L}{T_H}. \tag{59}$$

Therefore, although the cycle efficiency is independent of how $(\bar{h}A)$ is distributed among the two heat exchangers, the entropy generation rate per unit $(\bar{h}A)$ is minimized and the power output maximized when the cycle is positioned between T_H and T_L in the manner indicated by equations (57) and (58). The Brayton cycle occupies an increasingly taller area on the T–s diagram as M decreases, i.e. the number of heat transfer units of both heat exchangers increase.

CONCLUSION

This study showed that the degree of thermodynamic imperfection of power plants can be anticipated based on a very simple model that retains only three sources of heat transfer irreversibility: the hot-end heat exchanger, the cold-end heat exchanger and the direct heat leak to the ambient. If the designer maximizes the instantaneous power output then there are two important trade-offs to keep in mind, first, Curzon and Ahlborn's optimum Carnot temperature ratio and, second, the optimum balance between the sizes of the hot- and cold-end heat exchangers. There is also an interesting geometric construction for locating the optimum position of the power plant on the absolute temperature scale (Fig. 2). The efficiency of the power plant model is maximized if the available investment is distributed optimally between the jobs of building external conductance and internal resistance.

Overall, the study draws attention to the opportunity for using the most basic heat transfer modelling and analysis in order to describe the irreversible operation of admittedly complicated engineering systems. This approach is highlighted in a new treatise and graduate-level text on modern engineering thermodynamics [13].

Acknowledgement—This work was supported by the National Science Foundation (Thermal Systems and Engineering Program) through Grant No. CBT-8711369.

REFERENCES

1. A. Bejan, *Entropy Generation through Heat and Fluid Flow*, p. 181. Wiley, New York (1982).
2. F. L. Curzon and B. Ahlborn, Efficiency of a Carnot engine at maximum power output, *Am. J. Phys.* **43**, 22–24 (1975).
3. P. Salamon, A. Nitzan, B. Andresen and R. S. Berry, Minimum entropy production and the optimization of heat engines, *Phys. Rev.* **A21**, 2115–2129 (1980).
4. P. Salamon, Y. P. Band and O. Kafri, Maximum power from cycling a working fluid, *J. Appl. Phys.* **53**, 197–202 (1982).
5. P. Salamon and A. Nitzan, Finite time optimization of a Newton's law Carnot cycle, *J. Chem. Phys.* **74**, 3546 3560 (1981).
6. B. Andresen, P. Salamon and R. S. Berry, Thermodynamics in finite time, *Physics Today* 62–70 (September 1984).
7. A. De Vos, Efficiency of some heat engines at maximum-power conditions, *Am. J. Phys.* **53**, 570–573 (1985).
8. M. J. Moran, *Availability Analysis: a Guide to Efficient Energy Use*, Chap. 4. Prentice-Hall, Englewood Cliffs, New Jersey (1982).
9. T. J. Kotas, *The Exergy Method of Thermal Plant Analysis*, p. 73. Butterworths, London (1985).
10. D. B. Spalding and E. H. Cole, *Engineering Thermodynamics*, 3rd Edn, p. 209. Edward Arnold, London (1973).
11. G. M. Griffiths, CANDU—a Canadian success story, *Phys. Can.* **30**, 2–6 (1974).
12. A. Chierici, Planning of a geothermal power plant: technical and economic principles, U.N. Conference on New Sources of Energy, New York, Vol. 3, pp. 299–311 (1964).
13. A. Bejan, *Advanced Engineering Thermodynamics*. Wiley, New York (1988), and *Solutions Manual*.

THEORIE D'IRREVERSIBILITE DU TRANSFERT THERMIQUE APPLIQUEE A UN EQUIPEMENT ENERGETIQUE

Résumé—Le degré observé d'imperfection thermodynamique d'une installation est expliqué à partir d'un modèle en tenant compte des irréversibilités dues à trois sources : le côté chaud de l'échangeur, le côté froid et la chaleur se perdant dans l'ambiance. En optimisant la puissance instantanée délivrée, on montre qu'en plus du rapport de température optimum de Curzon et Ahlborn, il existe aussi un équilibre optimum entre les dimensions des extrêmités chaude et froide de l'échangeur. On présente une construction graphique de la position optimale de l'équipement énergétique dans l'échelle de température absolue. L'efficacité est maximale quand l'investissement total est séparé de façon optimale entre la conductance externe et la résistance thermique interne. Les données sur l'efficacité d'unités existantes tombent dans le domaine prévu théoriquement. Quelques points révélés par la théorie sont illustrés à travers l'analyse d'une installation fonctionnant selon un cycle idéal de Brayton.

THEORIE DER IRREVERSIBLEN WÄRMEÜBERTRAGUNG IN KRAFTWERKEN

Zusammenfassung—Der durch irreversible Vorgänge reduzierte Wirkungsgrad von Kraftwerken wird anhand eines stationären Modells untersucht. Es lassen sich dabei drei Quellen für Irreversibilitäten feststellen : die Wärmetauscher am heißen und kalten Ende der Anlage sowie der Wärmeverlust der Anlage an die Umgebung. Zur Optimierung der momentanen Energieausbeute wurde von Curzon und Ahlborn ein optimales Temperaturverhältnis ermittelt. Es wird gezeigt, daß zwischen der Größe der Wärmetauscher am heißen und kalten Ende ebenfalls ein optimales Verhältnis besteht. Ein Diagramm zur grafischen Ermittlung der optimalen Lage von Kraftwerken bezüglich der absoluten Temperaturskala wird vorgestellt. Der Wirkungsgrad (energetisch oder exergetisch) wird dann maximal, wenn die gesamten Anlagekosten optimal zwischen der Wärmedämmung nach außen und dem inneren thermischen Widerstand aufgeteilt werden. Die Daten über den Wirkungsgrad von bestehenden Kraftwerken fallen in den Bereich der Werte, die aufgrund der theoretischen Berechnungen zu erwarten sind. Einige der Verbesserungs-Möglichkeiten, die aufgrund der Theorie aufgedeckt worden sind, werden anhand der Analyse eines idealen Kraftwerks nach dem Brayton-Prozeß verdeutlicht.

ТЕОРИЯ ЭНЕРГОУСТАНОВКИ НА ОСНОВЕ НЕОБРАТИМЫХ ПРОЦЕССОВ ПЕРЕНОСА

Аннотация—Термодинамическая неидеальность существующих энергоустановок трактуется на основе модели стационарной энергоустановки, необратимый характер процессов в которой обязан трем причинам: теплообмену с нагревателем, с холодильником и утечкам тепла в окружающую среду. Путем максимизации значения выходной мгновенной мощности показано, что наряду с оптимальным отношением температур Керзона и Альборна существует также оптимальное отношение размеров нагревателя и холодильника. Разработан графический метод для определения оптимального расположения энергоустановки на абсолютной шкале температур. КПД (первый или второй законы) максимален, когда суммарный вклад оптимально распределен между внешней теплопроводностью и внутренним тепловым сопротивлением, встроенным в энергоустановку. Данные по КПД имеющихся энергоустановок совпадают с предсказанными теоретически. Некоторые пороговые значения, рассчитанные теоретически, иллюстрируются на идеальной машине с циклом Брайтона.